SUPPLEMENTAL INFORMATION FOR:

Oncogenic KRAS Reduces Expression of FGF21 in Acinar Cells to Promote Pancreatic Tumor Development in Mice on a High-Fat Diet

Yongde Luo[1,2,*], Yaying Yang[3, *], Muyun Liu[3,*], Dan Wang[2], Feng Wang[4], Yawei Bi[2], Juntao Ji[2], Suyun Li[2], Yan Liu[5], Rong Chen[6], Haojie Huang[5], Xiaojie Wang[1], Agnieszka K. Swidnicka-Siergiejko[5], Tobias Janowitz[7], Semir Beyaz[7], Guoqiang Wang[2], Sulan Xu[2], Agnieszka B. Bialkowska[2], Catherine K. Luo[2], Christoph L. Pin[8], Guang Liang[1], Xiongbin Lu[9], Maoxin Wu[10], Kenneth R. Shroyer[10], Robert A. Wolff[3], William Plunkett[6], Baoan Ji[11], Zhaoshen Li[12], Ellen Li[2], Xiaokun Li[1], Vincent W. Yang[2], Craig D. Logsdon[3,5,§], James L. Abbruzzese[3,13,§] & Weiqin Lu[2,3,§]

[1]School of Pharmaceutical Science, Wenzhou Medical University, Wenzhou, Zhejiang, China.

[2]Department of Medicine, [10]Department of Pathology, Stony Brook University, Stony Brook, NY, 11794, USA

[3]Department of Gastrointestinal Medical Oncology, [5]Department of Cancer Biology, [6]Department of Experimental Therapeutics, University of Texas, MD Anderson Cancer Center, Houston, TX, 77030, USA

[4]Sun Yat-Sen University Cancer Center, State Key Laboratory of Oncology in South China, Collaborative Innovation Center for Cancer Medicine, Guangzhou, 510060, China.

[7]Cold Spring Harbor Laboratory, Cold Spring Harbor, NY, 11724, USA

[8]Departments of Pediatrics, Oncology, and Physiology and Pharmacology, Schulich School of Medicine, University of Western Ontario Children's Health Research Institute, London, ON, Canada N5C 2V5

[9]Department of Medical and Molecular Genetics, Indiana University School of Medicine. Indianapolis, IN, USA

[11]Department of Biochemistry and Molecular Biology, Mayo Clinic, Jacksonville, FL, USA

[12]Department of Gastroenterology, Changhai Hospital, Shanghai, China

[13]Division of Medical Oncology, Department of Medicine, Duke Cancer Institute, Duke University, Durham, NC, 27710, USA

[*] Authors share co-first authorship.

[§]Authors share co-senior authorship

CONTENTS

1. Supplementary Figures

Supplementary Figure 1

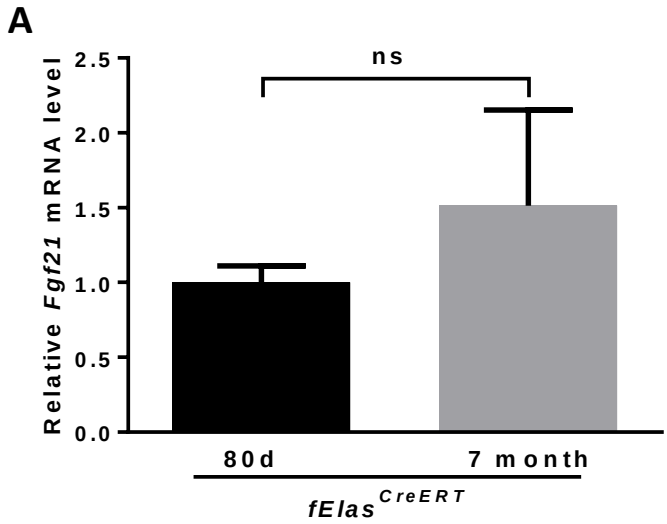

Supplementary Figure 1, relating to Figure 1. (A) qRT-PCR analysis of the expression levels of *Fgf21* in pancreatic tissues from 80-day-old *fElas*^{CreERT} mice (n=4) one week post-TM induction, and from 7-month-old *fElas*^{CreERT} mice (n=6) five months post-TM induction. All the mice were fed a normal diet for the duration of the experiments. Results indicate that pancreatic *Fgf21* gene expression remains

unchanged with age in the *fElas*^{CreERT} mice. Results are expressed as mean ± SD. *p* values are determined by the Student's *t*-test. ns, not significant.

Supplementary Figure 2

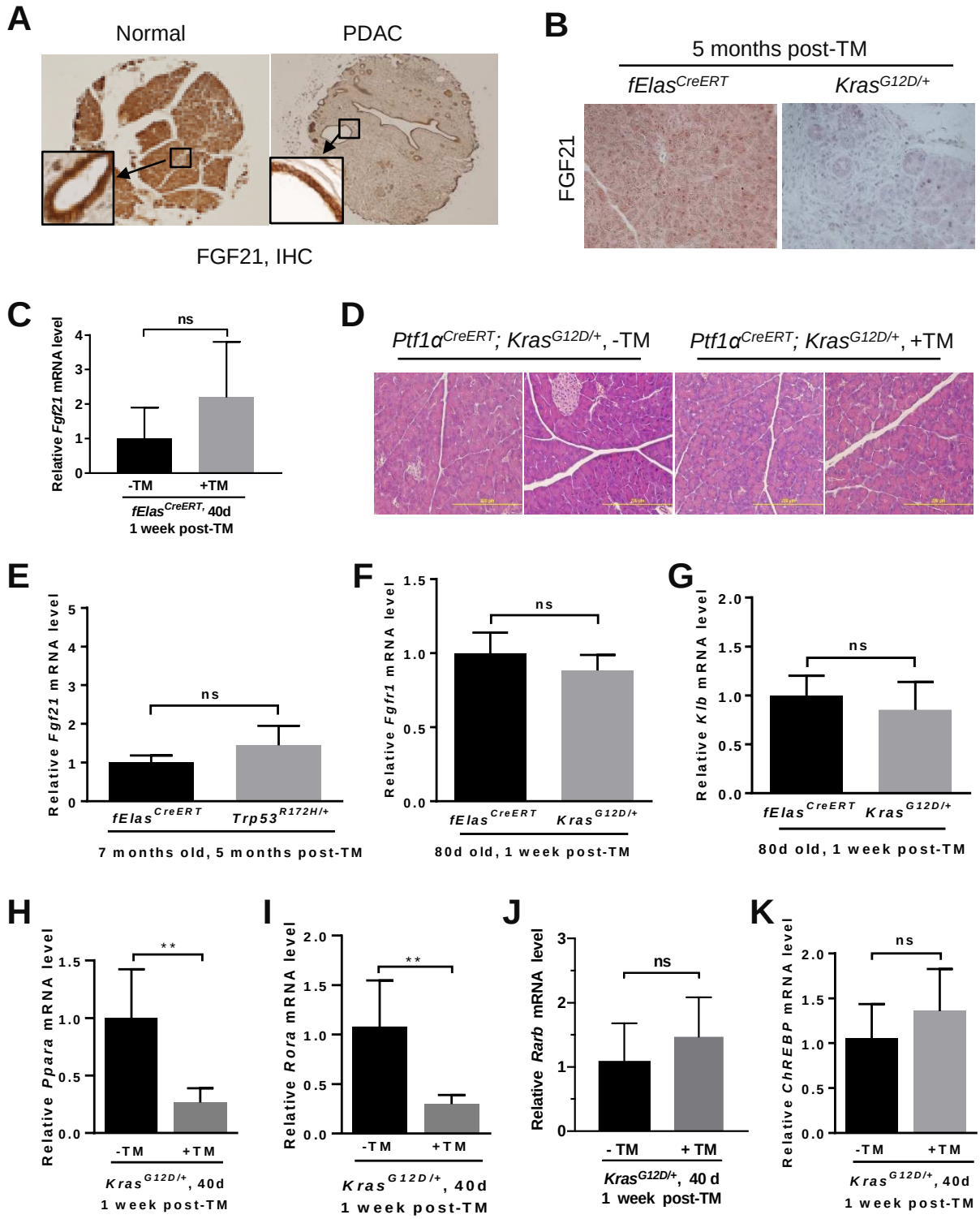

Supplementary Figure 2, relating to Figure 2. (A) Representative IHC staining of FGF21 in tissue arrays of normal human pancreata (left) and PDAC specimens (right) (40x). *Inset*: normal ducts, 200x. (B) Representative IHC analysis of FGF21 levels in 7-month-old $Kras^{G12D/+}$ mice 5 months post-TM induction. 200x. (C) qRT-PCR analysis for *Fgf21* expression in 40-day-old $fElas^{CreERT}$ mice one week after TM induction (n=11) or without TM induction (n=6). (D) Representative H&E staining of the pancreatic tissue sections in the $Ptf1\alpha^{CreERT};Kras^{G12D/+}$ mice with or without TM induction as in Figure 2H. (E) qRT-PCR analysis of *Fgf21* expression in pancreatic tissues obtained from 7-month-old $fElas^{CreERT}$ (n=3) and $Trp53^{R172H/+}$ (n=4) mice five months post-TM induction. (F) qRT-PCR analysis of pancreatic *Fgfr1* expression in 80-day-old $Kras^{G12D/+}$ mice (n=5) or $fElas^{CreERT}$ mice (n=4), one week post-TM treatment. (G) qRT-PCR analysis for pancreatic *Klb* expression in 80-day-old adult $Kras^{G12D/+}$ mice (n=9) or $fElas^{CreERT}$ mice (n=6), one week after TM treatment. (H-K) qRT-PCR analysis for pancreatic *Ppara, Rora, Rarb, and ChREBP* expression in 40-day-old $Kras^{G12D/+}$ mice (n=6) or $fElas^{CreERT}$ mice (n=6) one week post-TM induction. All the mice were fed a ND. Results are expressed as mean ± SD. *p* values are determined by the Student's *t*-test. ns: no significance. **, $p<0.01$.

Supplementary Figure 3

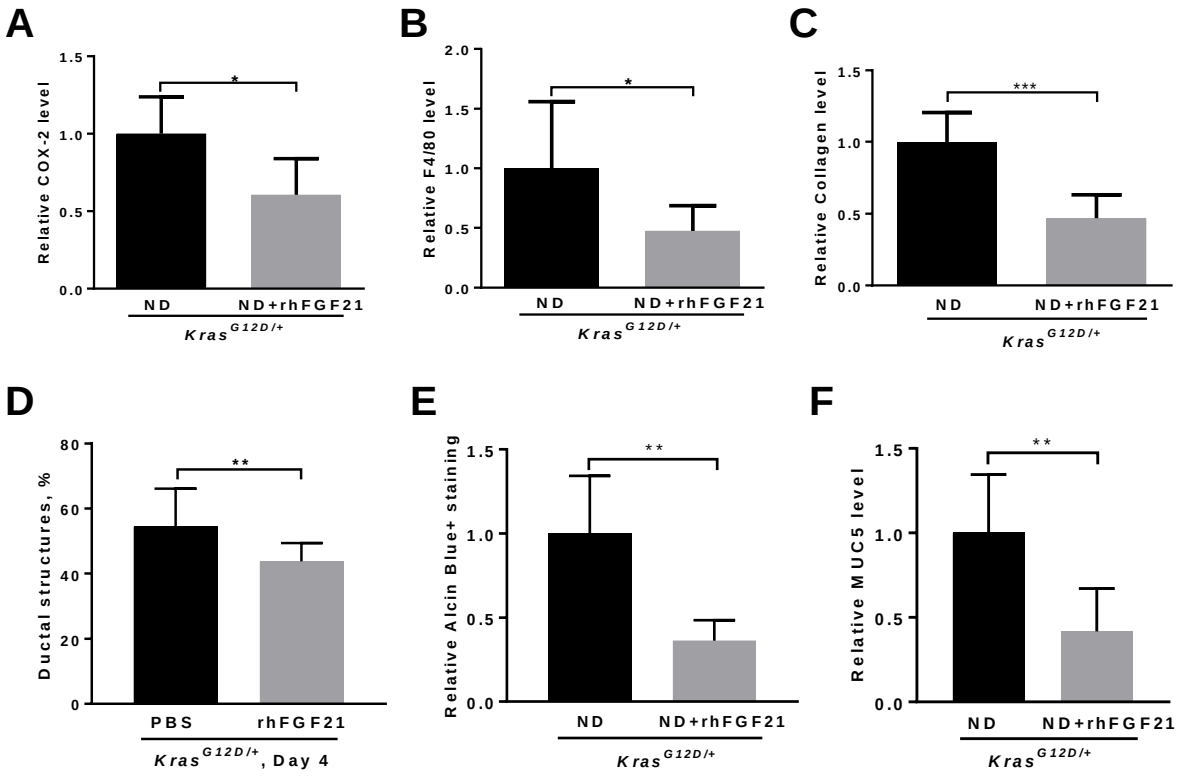

Supplementary Figure 3, relating to Figure 3. (A-B) Quantitative analysis of COX-2+ or F4/80+ areas in the *Kras*$^{G12D/+}$ mice with ND (n=4) or ND+rhFGF21 (n=4) treatment using images as represented in Figure 3B. (C) Quantitative analysis of Collagen+ areas in the *Kras*$^{G12D/+}$ mice with ND (n=6) or ND+rhFGF21 (n=5) treatment using images as represented in Figure 3B. (D) Quantification of the percentage of tubular ductal structures in the entire acinar clusters on day 4 after the indicated treatments with three independent experiments as shown in Figure 3F. (E) Quantitative analysis of Alcian blue+ areas over total areas in the *Kras*$^{G12D/+}$ mice with ND (n=6) or ND+rhFGF21 (n=6) treatment using images as represented in Figure 3G. (F) Quantitative analysis of MUC5+ areas in the *Kras*$^{G12D/+}$ mice with ND (n=5) or ND+rhFGF21 (n=5) treatment

using images as represented in Figure 3G. Fiji ImageJ software was used to obtain image data for statistical analyses. Results are expressed as mean ± SD. *p* values are determined by the Student's *t*-test. *, $p<0.05$; **, $p<0.01$; ***, $p<0.001$.

Supplementary Figure 4

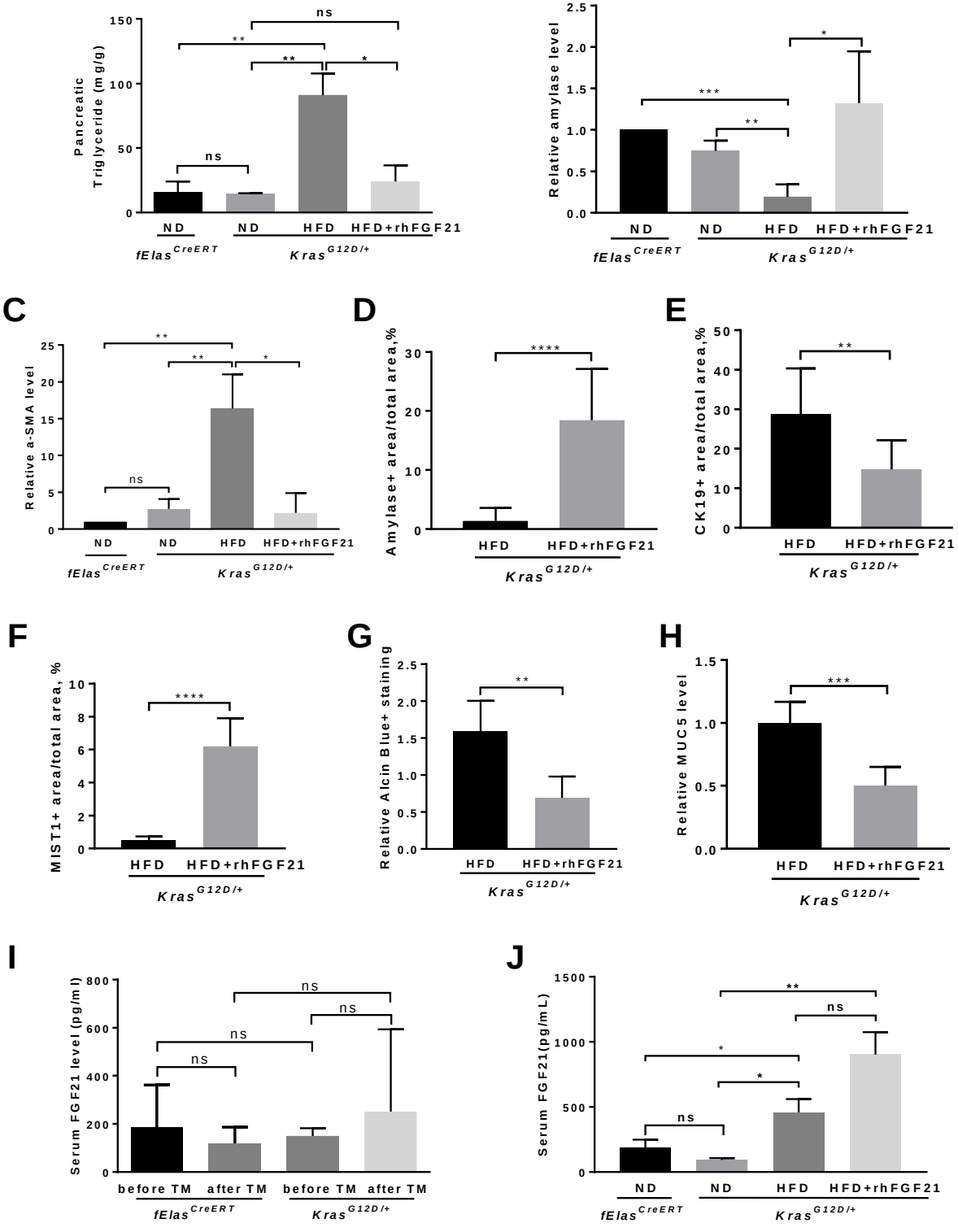

Supplementary Figure 4, relating to Figure 4. (A) Triglyceride levels in the pancreata were quantitatively analyzed in *Kras*$^{G12D/+}$ mice with the indicated treatments for 10 weeks. (B-C) Quantitative analysis of amylase or α-SMA protein levels from three independent Western blot data as represented in Figure 4E. (D-E) Quantitative analyses of amylase+ or CK19+ areas from the Co-IF imaging data from four different mice in each group as represented in Figure 4F. (F) Quantitative analysis of MIST1+ areas from IHC data of five different mice in each group as represented in Figure 4F. (G-H) Quantitative analysis of Alcian blue+ or MUC5+ areas over total areas using images after HFD (n=3) or HFD+rhFGF21 (n=3) treatment as represented in Figure 4G. (I) Serum FGF21 levels from the *fElas*^{CreERT} mice before (n=11) and one week post-TM treatment (n=11) and from the *Kras*$^{G12D/+}$ mice before (n=29) and one week post-TM treatment (n=31). Mice at 70 days of age were treated with TM and serum FGF21 levels were measured using Quantikine FGF21 ELISA kits. (J) 70-day-old *Kras*$^{G12D/+}$ and *fElas*^{CreERT} mice were treated with TM for 5 consecutive days followed by 10 weeks of the indicated treatments. Serum FGF21 levels were then compared using Quantikine FGF21 ELISA kits in the *Kras*$^{G12D/+}$ mice and the *fElas*^{CreERT} mice. Data from 4I and 4J suggest that pancreatic *Fgf21* gene silencing by Kras^{G12D} did not impact systemic FGF21 levels. No significant differences in serum FGF21 levels were observed in the HFD-fed *Kras*$^{G12D/+}$ mice regardless of rhFGF21 treatment, even though an increased tendency of serum FGF21 levels were observed in the group with concurrent HFD and rhFGF21 treatment, suggesting that rhFGF21 treatment did not significantly alter serum FGF21 levels. However, *Kras*$^{G12D/+}$ mice treated with either a HFD or HFD+rhFGF21 had significantly higher levels of serum FGF21 compared to that of the ND-fed

Kras$^{G12D/+}$ mice, suggesting that the increased serum FGF21 was induced mainly by HFD. Fiji ImageJ software was used to obtain data from IHC images for statistical analysis. Results are expressed as mean ± SD. *p* values are determined by the Student's *t*-test. ns, not significant, *, p<0.05; **, p<0.01; ***, p<0.001; ****, p<0.0001.

Supplementary Figure 5

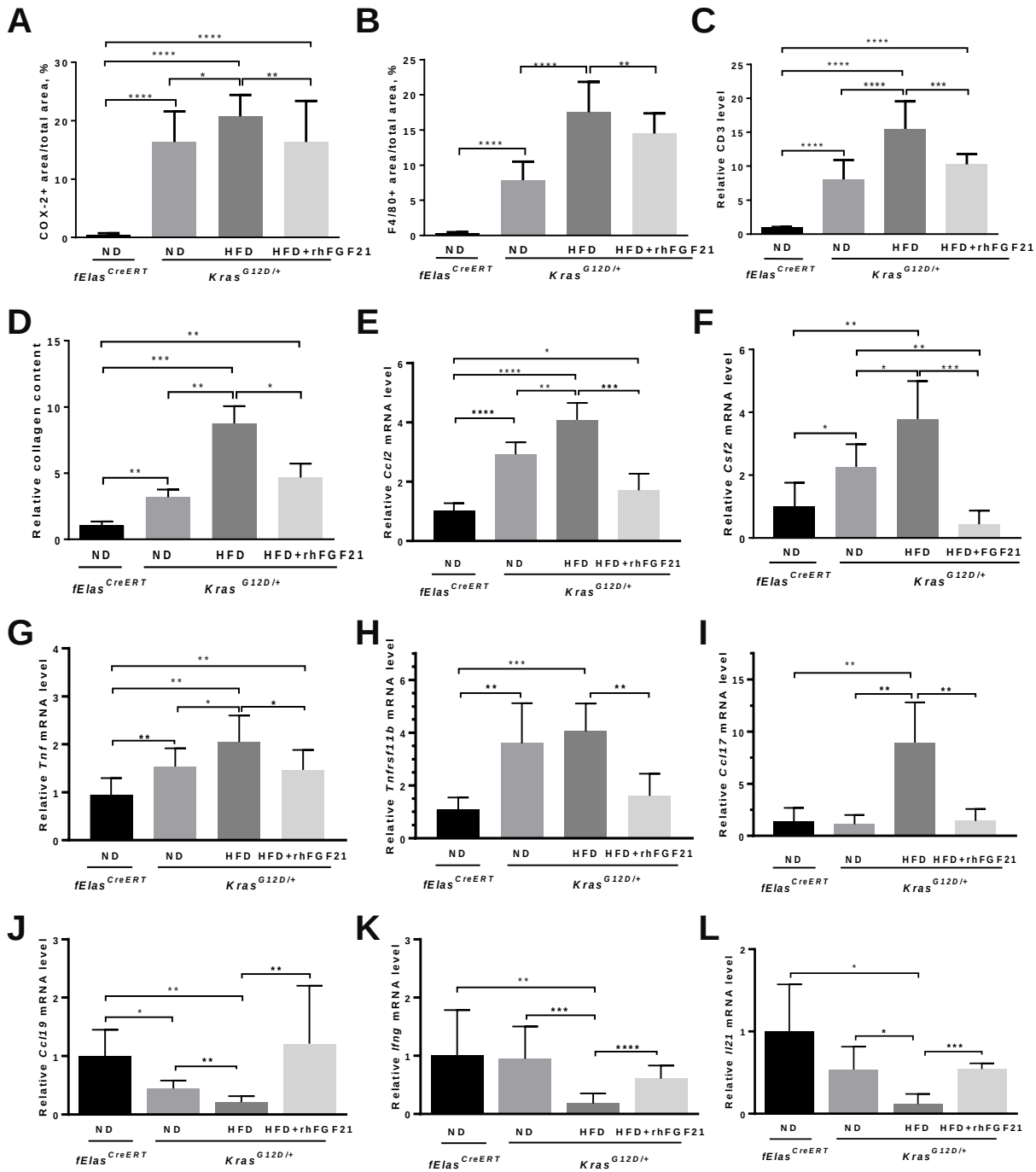

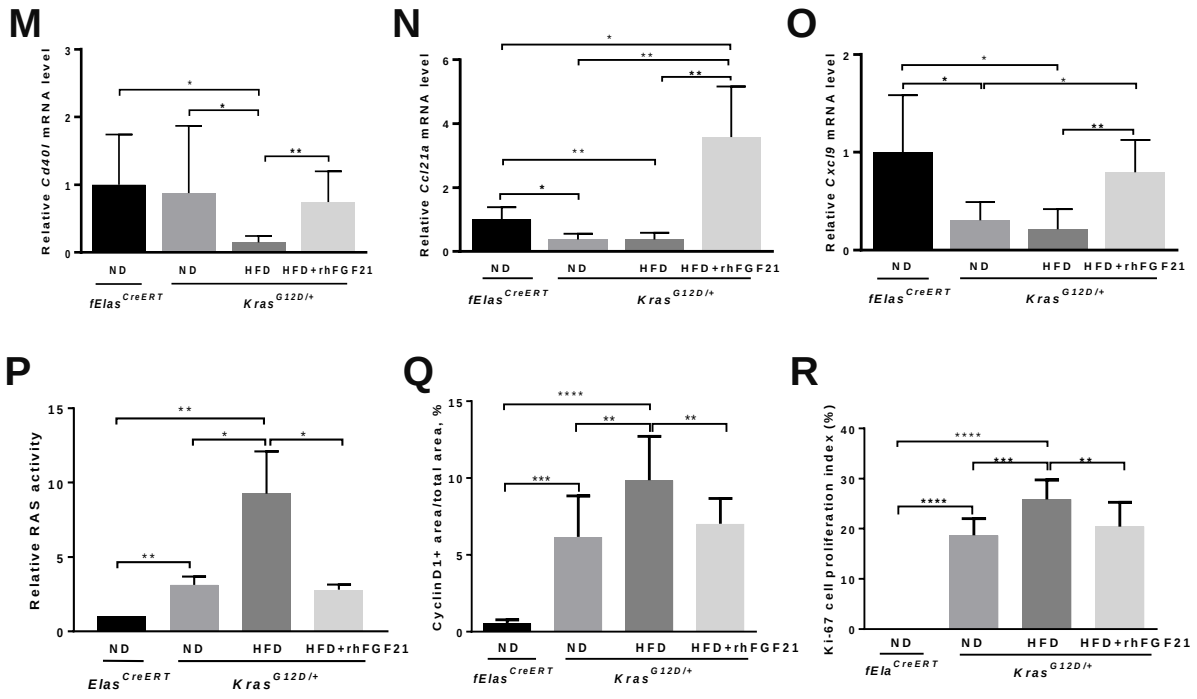

Supplementary Figure 5, relating to Figure 5. All tissue samples in the following analyses were described as in Figure 4A. The ND-fed *fElas*^{CreERT} mice (n=4) served as normal control. (A-D) Quantitative analysis of COX-2+, F4/80+, CD3+, and collagen-positive areas in *Kras*$^{G12D/+}$ mice with ND (n=4), HFD (n=4) or HFD+rhFGF21 (n=5) treatment as represented in Figure 5A. (E-O) qRT-PCR analysis of pancreatic *Ccl2, Csf2, Tnf, Tnfrsf11b, Ccl17*, *Ccl19*, *Ifng*, *Il21, Cd40l, Ccl21a, and Cxcl9* in the *Kras*$^{G12D/+}$ mice with ND (n=4), HFD (n=4) or HFD+rhFGF21 (n=5) treatment. (P) Quantitative analysis of pancreatic RAS activity from three independent RAS activity experiments as represented in Figure 5D. (Q) Quantitative analysis of Cyclin D1+ areas in the pancreata of *Kras*$^{G12D/+}$ mice with ND (n=4), HFD (n=4) or HFD+rhFGF21 (n=4) treatment as represented in the upper panel of Figure 5E. (R) Quantitative analysis of Ki-67+ areas in the pancreata of *Kras*$^{G12D/+}$ mice with ND (n=4), HFD (n=6) or

HFD+rhFGF21 (n=6) treatment as represented in the lower panel of Figure 5E. Fiji ImageJ software was used to obtain data from IHC images for statistical analysis. Results are expressed as mean ± SD. *p* values are determined by the Student's *t*-test. *, p<0.05; **, p<0.01; ***, p<0.001; ****, p<0.0001.

Supplementary Figure 6

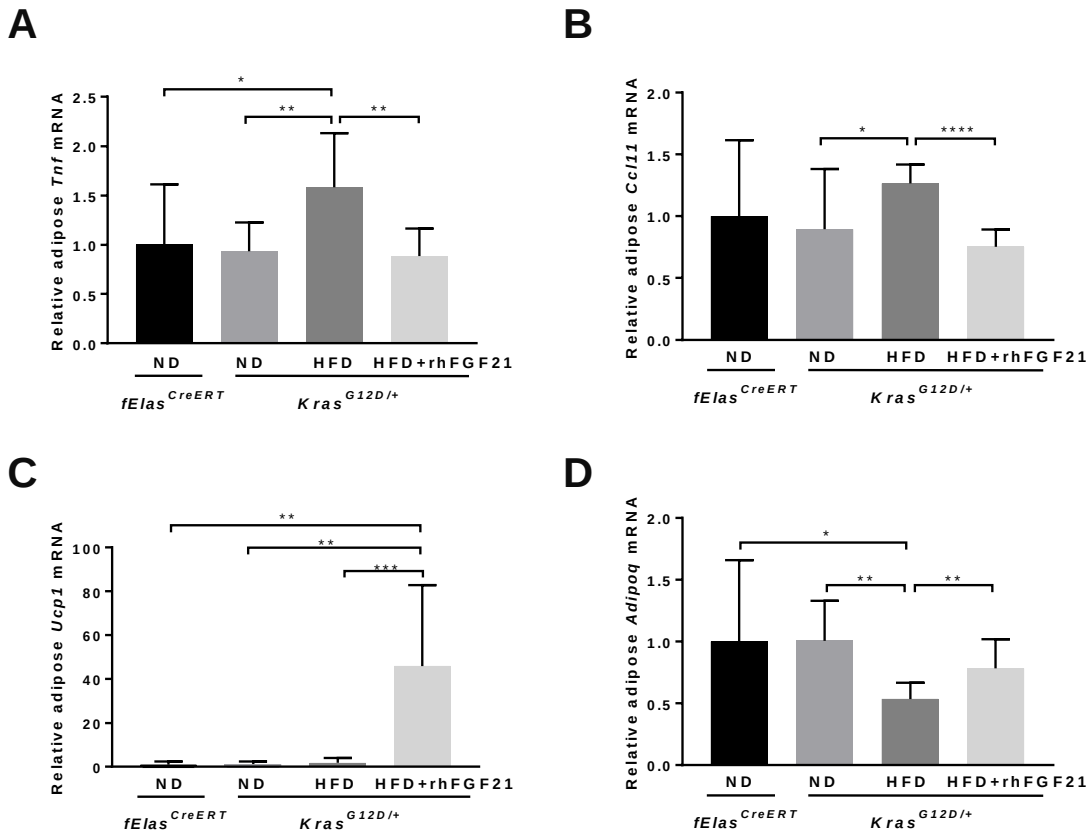

Supplementary Figure 6, relating to Figure 6. All mice were induced by TM at 70 days of age and then received the indicated treatments for 10 weeks prior to qRT-PCR analysis. (A-D) qRT-PCR analyses of adipose *Tnf, Ccl11, Ucp1,* and *Adipoq gene expression* in *Kras*$^{G12D/+}$ *mice* with ND (n=5), HFD (n=6) or HFD+rhFGF21 (n=5). The ND-fed *fElas*^{CreERT} mice (n=5) served as a control. Results are expressed as mean ± SD. *p* values are determined by the Student's *t*-test. *, p<0.05; **, p<0.01; ***, p<0.001; ****, p<0.0001.

Supplementary Figure 7

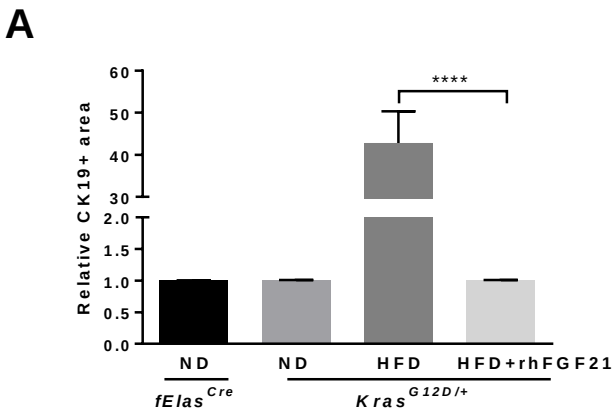

Supplementary Figure 7, relating to Figure 7. (A) Quantitative analysis of CK19+ areas in the representative liver images of *Kras*$^{G12D/+}$ mice with ND (n=4), HFD (n=6) or HFD+rhFGF21 (n=6) treatment as represented in Figure 7D (lower panel). Results are expressed as mean ± SD. *p* values are determined by the Student's *t*-test. ****, $p<0.0001$.

2. Supplementary Table 1

Supplementary Table 1. List of primer sets for qRT-PCR assessment of expression of different genes.

Gene symbol	Forward primer	Reverse primer
Fgf21	5'-TTCAAATCCTGGGTGTCAAA-3'	5'-CAGCAGCAGTTCTCTGAAGC-3'
h*FGF21*	5'-CGGGAGCTGCTTCTTGAGGA-3'	5'-CTGGTAGTGGCAGGAAGCGA-3'
Fgfr1	5'-CTGAAGGAGGGTCATCGAAT-3'	5'-GTCCAGGTCTTCCACCAACT-3'
Klb	5'-CAGAGAAGGAGGAGGTGAGG-3'	5'-CAGCACCTGCCTTAAGTTGA-3'
β-actin	5'-CGGTTCCGATGCCCTGAGGCTCTT-3'	5'-CGTCACACTTCATGATGGAATTGA-3'
18S rRNA	5'-GCAATTATTCCCCATGAACG-3'	5'-GGCCTCACTAAACCATCCAA-3'
Cxcl5	5'-GGAGCTGCGTTGTGTTTGCT-3'	5'-ACTTCCACCGTAGGGCACTG-3'
Tgfβ1	5'-CCCGTGGCTTCTAGTGCTGA-3'	5'-ACAGGATCTGGCCACGGATG-3'
Ccl2	5'-GCATCTGCCCTAAGGTCTTC-3'	5'-AAGTGCTTGAGGTGGTTGTG-3'
Csf2	5'-TTTACTTTTCCTGGGCATTG-3'	5'-TAGCTGGCTGTCATGTTCAA-3'
Tnf	5'-ATGAGAAGTTCCCAAATGGC-3'	5'-CTCCACTTGGTGGTTTGCTA-3'
Ccl17	5'-CCGAGAGTGCTGCCTGGATT-3'	5'-GAGCTTGCCCTGGACAGTCA-3'
Ccl19	5'-TCAGCTCTGTGCACCTCCAG-3'	5'-GCTCCTTCTGGTGCTGTTGC-3'
Tnfrsf11b	5'-CATCTCGGCCACTCGAACCT-3'	5'-AGGAGCTGCTCGCTCGATTT-3'
Ccl4	5'-AGCAACACCATGAAGCTCTG-3'	5'-CCGGGAGGTGTAAGAGAAAC-3'
CD68	5'-CCGGACCCACAACTGTCACT-3'	5'-GAGGGCCAACAGTGGAGGAT-3'
CD11b	5'-GCCTCCCTTTGCTCTGTGGA-3'	5'-CTCGAGGCAAGGGACACACT-3'
Ucp1	5'-CTCGAGGCAAGGGACACACT-3'	5'-AAAGGACTCAGCCCTGAAGA-3'
Ifng	5'- CATTCAGAGCTGCAGTGACC-3'	5'- CTGTCTGGCCTGCTGTTAAA-3'
Il21	5'-GGCCATTCCCACTCCCATCT-3'	5'-TTCTGCGCACTGAGGAGAGG-3'
Cd40l	5'-AGGCGGCAAATACCCACAGT-3'	5'-TGGCTTGCTTCAGTCACGTTG-3'
Ccl21a	5'-GCTCCAAGGGCTGCAAGAGA-3'	5'-TTGCCTGTGAGTTGGACCGT-3'
Cxcl9	5'-TCTGCCATGAAGTCCGCTGT-3'	5'-GCAGGAGCATCGTGCATTCC-3'
Adipoq	5'- AAGGCCGTTCTCTTCACCTA-3'	5'-TACACCTGGAGCCAGACTTG-3'
Pparg	5'-TTCTGCGCACTGAGGAGAGG-3'	5'-AGACTCTGGGTTCAGCTGGT-3'
Ppara	5'-AGACTCTGGGTTCAGCTGGT-3'	5'-GAAGCTGGAGAGAGGGTGTC-3'
Rorα	5'-ACTTGCGGGAAGAGCTCCAG-3'	5'-CACACAGCTGCCACATCACC-3'

Note: Primer sets were designed at https://www.genscript.com/tools/real-time-pcr-taqman-primer-design-tool. The parameters used include the minimum Tm 58^{o}C, optimum Tm 59^{o}C, maximum Tm 60^{o}C, primer length 16-20 bp, amplicon size 90-150 bp. Primer crossing exon junction is not allowed. h=human.

3. Supplementary Materials and Methods

The details of other materials and methods used throughout the study include (1) Animal treatment; (2) Production of recombinant FGF21; (3) Cell culture; (4) Histology analysis; (5) Immunohistochemistry and immunofluorescence; (6) Analysis of FGF21 levels on human pancreatic tissue array; (7) Pancreatic fibrosis; (8) PanIN quantification; (9) Ki-67 proliferation index; (10) Protein isolation and Western blot analysis; (11) RAS activity assay; (12) Gene expression analysis; (13) Triglycerides content in the pancreas; (14) Pancreatic acini extraction and 3-dimensional culture; (15) Serum FGF21 levels; (16) Statistical analysis.

Animal treatment

fElas^{CreERT}, *fElas*^{CreERT};*Kras*$^{LSL\text{-}G12D/+}$, *Ptf1a*^{CreERT};*Kras*$^{LSL\text{-}G12D/+}$, and *fElas*^{CreERT};*Trp53*$^{LSL\text{-}R172H/+}$ mice, including both male and female, were randomly recruited and given TM by peritoneal injection for five consecutive days to fully activate Cre recombinase in acinar cells. According to the treatment plan, *Kras*$^{G12D/+}$ and *fElas*^{CreERT} mice were fed with either normal laboratory supplied diet or high-fat diet (60% fat, Test Diet DIO 58Y1 van Heek Series; Lab Supply, Fort Worth, TX). The mice were given rhFGF21 at 0.5 mg/kg/day as described[1, 2]. Phosphate-buffered saline (PBS) of the same volume was used as an experimental control. Body weight of each mouse was measured at least once a week. After about ten weeks of treatment or due to tumor burden requiring a humane sacrifice, mice were euthanized, and the pancreas, liver, spleen, blood, and/or fat tissues were harvested for further experiments.

Production of recombinant FGF21

Recombinant 6 x His-tagged human FGF21 for *in vivo* injection was produced in *E. coli* BL21 DE3 and purified as described[3].

Cell culture

Panc-1, MIA Paca-2, SU86.86, and AsPC-1 cells were cultured in RPMI 1640 or DMEM media supplemented with 10% FBS, as well as penicillin and streptomycin. All these cell lines were obtained from American Type Culture Collection (ATCC) and proven to carry oncogenic *KRAS.* HPDE cells were cultured in serum-free keratinocyte (KSF) medium supplemented by epidermal growth factor and bovine pituitary extract (Life Technologies, Inc., Grand Island, NY).

Histology analysis

Mouse tissues were dissected, rinsed with PBS, and fixed in 10% formalin solution overnight. Formalin-fixed tissue samples were placed in cassettes, dehydrated in alcohol gradients, and then embedded in paraffin for sectioning. The 5-μm-thick tissue sections were dewaxed in xylene, rehydrated through reversed ethanol gradients, washed in PBS thoroughly, and then stained with H&E. After staining, the pathological changes in pancreatic tissues were evaluated by our experienced pathologists based on criteria described at http://pathology.jhu.edu/pc/professionals/DuctLesions.php. PDAC incidences were also assessed by two independent pathologists.

Immunohistochemistry and immunofluorescence

To evaluate the levels of representative protein makers, including COX-2, FGF21, KLB, F4/80, Ki-67, Cyclin D1, amylase, CD3, and CK19, immunohistochemical and immunofluorescent analyses were performed as described[4, 5]. Briefly, after deparaffinized in xylene, rehydrated in alcohol gradients and rinsed with PBS, tissue sections were subjected to heat-mediated antigen retrieval with citrate buffer (pH 6.0) and then treated with 0.5% H_2O_2 in methanol for 10 min to remove the endogenous peroxidase followed by blocking with normal serum. The treated sections were then incubated with primary antibodies against COX-2 (1:20, Thermo), FGF21 (1:200, Abcam), KLB (1:200, Abcam), F4/80 (1:100, eBioscience), Ki-67 (1:200, Thermo), Cyclin D1 (1:200, Santa Cruz), amylase (1:400, Santa Cruz), and CK19 (1:50, Santa Cruz) at 4℃ overnight. After washing, the sections were further incubated with the appropriate biotinylated secondary antibodies (Vector Laboratories, CA, USA) at room temperature for 1 hr, washed again in PBS, incubated with ABC reagent (Vector Laboratories, CA, USA) for 30 min, and then reacted with diaminobenzidine (DAB, Vector Laboratories, CA, USA) for about 3 min. The resulting sections were then counterstained with hematoxylin until the desired stain intensity developed. Immunofluorescence was performed as described[4, 5]. Fiji ImageJ software was used to obtain data from most IHC images for quantification and statistical analyses.

Analysis of FGF21 levels on human pancreatic tissue array

Human normal (n=45) and PDAC (n=59) pancreatic tissue array samples (US Biomax, MD, USA) were processed for IHC analysis on FGF21 expression. Positive FGF21

expression was defined as the presence of cytoplasm staining in cells. Tissue cores containing tumor foci in less than 10% of the whole area were excluded from evaluation. Relative FGF21 levels were scored as the product of a proportion score and an intensity score. The proportion score was determined by the fraction of positively stained neoplastic cells (0, none; 1, <10%; 2, 10–50%; 3, 51–80%; 4, >80%). The intensity score represented the staining intensity (0 = negative, 1 = weak, 2 = moderate, 3 = strong). Mean staining intensity of three tumor cores per patient on the tissue array was calculated for each case.

Pancreatic fibrosis

To evaluate pancreatic fibrosis, we analyzed the levels of pancreatic collagen using Sirius Red staining on pancreatic tissue sections. Briefly, tissue sections were deparaffinized, hydrated in ethanol gradients and distilled water, and then incubated in adequate Picro-Sirius Red Solution (Abcam, MA, USA) for 60 minutes. After rinsing quickly in two changes of acetic acid solution followed by dehydration with two changes of absolute alcohol, the Sirius Red-stained sections were sealed and photographed under light microscopes. Three digitized pictures of each pancreatic section were photographed using an Olympus iX81 microscope at 200x magnification. The images were analyzed using Fiji ImageJ software. Levels of pancreatic collagen deposition were presented as the ratio of the mean collage-stained area to the whole mean area of the section and finally converted to relative collagen contents.

PanIN quantification

The H&E stained pancreatic sections were histologically evaluated by two independent pathologists blinded to the experimental groups according to histopathology criteria as recommended[6]. Each lobule of the pancreas on each section was examined, and the highest grade lesion from each lobule was identified, and the percentage of lobules with the highest grade of each type of lesion was determined based upon the total number of lobules counted.

Ki-67 proliferation index

Ki-67 proliferation index was determined as the percentage of positively stained cell nuclei of neoplastic cells. 5-10 random fields were chosen per tissue section (200x). Non-neoplastic cells such as lymphocytes and endothelial cells were excluded for counting[7].

Protein isolation and Western blot analysis

To evaluate protein levels of amylase, α-SMA, FGF21, KLB, GAPDH, and β-actin, cell and tissue lysates were separated by SDS-PAGE and analyzed by immunodetection as described[8]. Briefly, snap-frozen tissues were homogenized in 0.5-1 ml ice-cold lysis buffer (Millipore, MA, USA) with protease inhibitor cocktail tablets (Roche, Germany). Tissue homogenates were centrifuged at 15,000 g for 15 minutes at 4℃, and the supernatant was collected. Protein lysates from tissue were aliquoted to determine protein concentration using a protein assay dye reagent concentrate (Bio-Rad, CA, USA). The lysates were separated by SDS-PAGE and then transferred to nitrocellulose membranes [8]. The membranes were rinsed with PBS containing 0.05% Tween 20

(PBS-T) and probed with the following antibodies against amylase (1:20000; Santa Cruz Biotechnology Inc.), α-SMA (1:400; Abcam), FGF21 (1:1000; Abcam), KLB (1:2000, R&D), GAPDH (1:10,000; Sigma-Aldrich), and β-actin (1:10000, Sigma-Aldrich). The membranes were then washed with PBS-T and probed with the respective secondary antibodies conjugated to horseradish peroxidase or Alexa-Fluor 800 or 680 for one hour at room temperature. Autoradiography or the Odyssey Imaging System (LiCor Biosciences, Lincoln, NE) was used to visualize protein bands. Stripping buffer (Thermo, MA, USA) was used for sequential blotting and reprobing with other antibodies to provide a loading control. ImageJ densitometry software was used to quantify individual bands.

RAS activity assay

Levels of GTP-occupied RAS from mice pancreatic lysates were measured using a RAF pull-down assay kit (Millipore, MA, USA) as previously described[9]. Briefly, snap-frozen pancreatic tissues were homogenized on ice in lysis buffer. Cellular debris was removed by centrifuging at 15,000g for 20 minutes at 4℃. P rotein concentrations were measured. About 1000 μg of lysates were incubated for 50 minutes at 4℃ w ith agarose beads coated with RAF-RBD domain, which can specifically pull-down the GTP-bound form of Ras proteins. The beads were then washed for 3 times with washing buffer. Active RAS was analyzed by immunoblotting with an anti-RAS primary antibody (1:2000, Millipore) using GAPDH as a sample loading control. The intensity of the bands generated from Western blot assay was quantified using ImageJ software, and the fold changes relative to RAS activity from *fElas*^{CreERT} mice were determined.

Gene expression analysis

The gene expression of *Fgf21*, *Klb*, *Fgfr1,* multiple inflammatory cytokines (Inflammatory Cytokines and Receptors PCR Array, Qiagen) and multiple FGF21-regulating transcription factors relative to *β-actin* and *18S rRNA* (Supplementary Table 1) were analyzed by qRT-PCR. Total RNA isolation, 1st strand cDNA synthesis, semi-quantitative PCR, and qPCR were performed as described[8]. Briefly, tissues or cells were homogenized in 1 ml TRIzol Reagent (Ambion, Life Technologies, CA), total RNAs were further separated from other cell contents by sequential chloroform and isopropanol precipitation. Aliquots of RNA samples were quantified and examined before reverse transcription using a Nanodrop to verify that there was no contamination with protein and genomic DNA. Semi-quantitative RT-PCR products after 32 cycles were analyzed by agarose gel electrophoresis. Inflammatory cytokine gene arrays (Inflammatory Cytokines and Receptors PCR Array, Qiagen) were first used to determine by qRT-PCR the changes in gene expression of inflammatory cytokines/chemokines and receptors. Gene expressions of statistically significant alterations were then individually confirmed by qRT-PCR using primer sets as listed in Supplementary Table 1, in the Quantifast SYBR Green PCR mix (Qiagen GmbH, Germany) with a reaction condition of initial denaturation at 95^{o}C for 5 min and then 40 cycles of 95^{o}C for 10 seconds and 60^{o}C for 30 seconds in QuantStudio 3 machine. The comparative threshold Ct method was used with *β-actin* and *18S rRNA* as internal references. Data quantification and statistic analysis were performed in Microsoft Excel and GraphPad Prism 6.0.

PPARG activation and FGF21 expression

To evaluate the effect of PPARG activation on pancreatic *FGF21* expression, we utilized the mutant *KRAS*-harboring Panc-1 cells. These cells were freshly cultured in RPMI-1640 media containing 10% FBS in 6-well plates at equal cell density. When reaching subconfluent (about 80%), these cells were treated with Rosiglitazone at concentrations of 0, 0.1, 1, and 10 μM for 18 hours. Cells were washed once with warm 1 x PBS, and total RNA was extracted for qRT-PCR analysis as described above.

Triglycerides content in the pancreas

Triglyceride colorimetric assay kit (Cayman Chemical Company, MI, USA) was used to determine the triglycerides content in the pancreas. 500 mg of fresh pancreatic tissues were minced into small pieces and homogenized in 2 ml of diluted Standard Diluent containing protease inhibitor cocktail tablets (Roche, Germany). The homogenates were then centrifuged at 10,000 x g for 10 minutes at 4°C, and the supernatant was transferred to another tube. An appropriate volume of samples was added to the designated wells on the plate according to the protocol. Reactions were initiated by adding the corresponding diluted enzyme solution. After incubating for 15 minutes at room temperature, the absorbance of the reaction was determined at 530-550 nm on a plate reader.

Pancreatic acini extraction and 3-dimensional culture

Pancreatic acini were prepared as described previously[10], seeded in collagen containing 24-well plates, cultured, treated daily with rhFGF21 (1 μg/ml) or PBS, and stained with H&E or co-immunofluorescent probes as described[10-12]. Three independent experiments were performed.

Serum FGF21 levels

Mouse whole blood samples were collected in clean 1.5 ml Eppendorf centrifuge tubes. For rhFGF21 treatment groups, blood samples were collected 24 hrs after rhFGF21 injection. Tubes with blood samples were placed on ice for 30 min without any disturbance. Blood samples were then centrifuged at 3,000 rpm for 10 min at 4℃, and the supernatants were harvested and stored at −80℃ until analyzed. Serum FGF21 concentrations were measured using Rat/Mouse (#MF2100) FGF21 enzyme-linked immunosorbent assay (ELISA) kits (Quantikine ELISA; R&D Systems, Minneapolis, MN, USA).

Statistical analysis

Comparison between two groups was analyzed by Student's *t*-test unless otherwise indicated. Log-rank (Mantel-Cox) test, based on the Log-rank statistic, was performed to determine the significant differences between two or more survival curves. The body weight data were analyzed by two-way ANOVA Tukey's multiple comparisons test. *p* values of less than 0.05 were considered to be statistically significant. Results were expressed as group mean ± SEM or mean ± SD. **, p*<0.05; **, *p*<0.01; ***, *p*<0.001; ****, *p*<0.0001. ns, not significant. We used GraphPad Prism 6.0 for statistical analysis.

References

1. Adams AC, Yang C, Coskun T, et al. The breadth of FGF21's metabolic actions are governed by FGFR1 in adipose tissue. Mol Metab 2012;2:31-7.
2. BonDurant LD, Ameka M, Naber MC, et al. FGF21 Regulates Metabolism Through Adipose-Dependent and -Independent Mechanisms. Cell Metab 2017;25:935-944 e4.
3. Yang C, Jin C, Li X, et al. Differential specificity of endocrine FGF19 and FGF21 to FGFR1 and FGFR4 in complex with KLB. PLoS One 2012;7:e33870.
4. Siveke JT, Einwachter H, Sipos B, et al. Concomitant pancreatic activation of Kras(G12D) and Tgfa results in cystic papillary neoplasms reminiscent of human IPMN. Cancer Cell 2007;12:266-79.
5. Kopp JL, von Figura G, Mayes E, et al. Identification of Sox9-dependent acinar-to-ductal reprogramming as the principal mechanism for initiation of pancreatic ductal adenocarcinoma. Cancer Cell 2012;22:737-50.
6. Hingorani SR, Petricoin EF, Maitra A, et al. Preinvasive and invasive ductal pancreatic cancer and its early detection in the mouse. Cancer Cell 2003;4:437-50.
7. Khan MS, Luong TV, Watkins J, et al. A comparison of Ki-67 and mitotic count as prognostic markers for metastatic pancreatic and midgut neuroendocrine neoplasms. Br J Cancer 2013;108:1838-45.

8. Lu W, Hu Y, Chen G, et al. Novel role of NOX in supporting aerobic glycolysis in cancer cells with mitochondrial dysfunction and as a potential target for cancer therapy. PLoS Biol 2012;10:e1001326.
9. Huang H, Daniluk J, Liu Y, et al. Oncogenic K-Ras requires activation for enhanced activity. Oncogene 2014;33:532-5.
10. Gruber R, Panayiotou R, Nye E, et al. YAP1 and TAZ Control Pancreatic Cancer Initiation in Mice by Direct Up-regulation of JAK-STAT3 Signaling. Gastroenterology 2016;151:526-39.
11. Qu C, Konieczny SF. Pancreatic Acinar Cell 3-Dimensional Culture. Bio Protoc 2013;3.
12. Shen J, Ha DP, Zhu G, et al. GRP78 haploinsufficiency suppresses acinar-to-ductal metaplasia, signaling, and mutant Kras-driven pancreatic tumorigenesis in mice. Proc Natl Acad Sci U S A 2017;114:E4020-E4029.